Coherent Multicarrier Receiver for Mobile Acoustic Channels

Amir Tadayon, *Graduate Student Member, IEEE* and Milica Stojanovic, *Fellow, IEEE*
Northeastern University, Boston, MA, USA

***Abstract*—High data rate coherent communication in acoustic channels are difficult due to the compound effects of motion-induced Doppler and long multipath. To account for these effects, we consider a coherent receiver based on orthogonal frequency division multiplexing (OFDM) which performs an iterative frequency offset compensation and sparse channel estimation. In mobile acoustic systems, Doppler effect can be severe enough that the OFDM signals experiences non-negligible frequency offsets even after initial resampling. To compensate for these offsets, a practical method based on stochastic gradient is employed. The method relies on differential encoding which keeps the receiver complexity at a minimum and requires only a small pilot overhead. Differential encoding is applied across carriers, promoting the use of a large number of closely spaced carriers within a given bandwidth. This approach simultaneously supports frequency domain coherence and efficient use of bandwidth for achieving high bit rates. After compensating for the frequency offset, a sparse channel estimation method based on a physical model of multipath propagation is used to obtain channel state information for coherent detection. The channel estimation method, referred to as path identification (PI), targets the physical propagation *paths* in a continuous-delay domain, and focuses on explicit estimation of delays and complex amplitudes of the channel paths in an iterative fashion. Using the experimental data transmitted over a 3-7 km shallow water channel in the 10.5-15.5 kHz acoustic band, we study the receiver performance in terms of data detection mean squared error (MSE) and bit error rate (BER), and show that the proposed receiver provides excellent performance at low computational cost.**

I. Introduction

High data rate coherent transmission over acoustic channels is a challenging problem due to the combined effects of long multipath and Doppler fluctuations. To account for these effects, we consider a coherent receiver based on multicarrier modulation in the form of orthogonal frequency division multiplexing (OFDM). OFDM is an attractive method for data transmission over frequency-selective channels due to its ability to achieve high bit rates at reasonably low computational loads. This fact motivates the use of OFDM in mobile acoustic communications where the channel exhibits long multipath delays but each narrowband carrier only experiences flat fading, thus eliminating the need for time-domain equalizers [1]–[3].

Applying OFDM to acoustic channels is made difficult by its sensitivity to the Doppler distortion caused by relative motion between the transmitter and receiver, which results in frequency shifting. For the relative transmitter/receiver velocity v and the propagation speed c (nominally 1500 m/s), Doppler scaling occurs at the rate $a = v/c$. In highly mobile scenarios, where v is on the order of a few m/s, Doppler frequency scaling is effectively seen as a time-varying channel distortion which adversely affects the performance of OFDM systems as it causes loss of orthogonality between the carriers. To mitigate the resulting distortion, front-end resampling must be performed [1]–[3]. Since coarse resampling is typically performed on an entire frame of OFDM blocks, each block within a frame may still experience different frequency offsets. We target these frequency offsets through a stochastic gradient approach as an iterative version of the hypothesis testing method proposed in [4]. The approach is based on differentially encoding which keeps the receiver complexity at a minimum and requires only a very low pilot overhead. Differential encoding is applied across carriers, promoting the use of a large number of carriers within a given bandwidth [3].

Coherent detection of OFDM signals requires the knowledge of channel coefficients in the frequency domain. To estimate the channel coefficients, in this paper, we formulate the problem of sparse channel estimation in a manner that capitalizes on a physical model of multipath propagation. The resulting approach, termed path identification (PI), targets a continuum of path delays, eliminating the conventional sample-spaced models and focusing instead on processing a transformed version of the signal observed over all the carriers spanning the system bandwidth. The PI algorithm focuses on explicit estimation of delays and complex amplitudes of the channel paths. Unlike the sparse identification methods [5], [6], the resolution and coverage in delay that the PI method provides can be increased arbitrarily without a prohibitive cost to complexity [7].

While [7], [8] illustrate the benefits of the frequency offset and channel estimation algorithms separately, in this paper we consider these algorithms operating in tandem and demonstrate their performance on experimental data from the Mobile Acoustic Communication Experiment (MACE 2010) showing excellent results. In the MACE'10 experiment, OFDM blocks containing 1024 8-PSK modulated carriers, which occupy the acoustic frequency range 10.5-15.5 kHz, were transmitted over a long-range (3-7 km) shallow water channel (about 100 m deep) and received over a 12-element vertical array spanning a total linear aperture of 1.32 m. The results lead us to conclude that the proposed coherent receiver is especially well-suited for implementation in acoustic multicarrier systems.

The rest of the paper is organized as follows. In Sec. II, we introduce the signal, system and channel model. Sec. III discusses the receiver algorithms used for coherent detection. Sec. IV contains the results of experimental data processing. Sec.V contains the conclusions.

II. Signal, System and Channel Model

We consider an OFDM system with M_r equi-spaced receivers and K carriers within a total bandwidth B. Let f_0 and $\Delta f = B/K$ denote the first carrier frequency and carrier spacing, respectively. We assume the use of zero-padding at the transmitter along with the overlap-and-add procedure at the receiver. The transmitted OFDM block is then given by

$$s(t) = Re\left\{\sum_{k=0}^{K-1} d_k e^{2\pi i f_k t}\right\}, \quad t \in [0,\ T] \tag{1}$$

where $T = 1/\Delta f$ is the OFDM block duration. The data symbol d_k, which modulates the k-th carrier of frequency $f_k = f_0 + k\Delta f$, belongs to a unit-amplitude phase shift keying alphabet (PSK).

The transmitted signal passes through M_r multipath acoustic channel whose impulse responses can be modeled as

$$h_m(\tau, t) = \sum_p h_p^m(t)\delta(\tau - \tau_p^m(t)) \tag{2}$$

where $h_p^m(t)$ and $\tau_p^m(t)$ represent the gain and delay of the pth path, respectively. We isolate a common Doppler scaling factor a such that $\tau_p^m(t) \approx \tau_p^m - at$, and further assume that the path gains are slowly varying such that $h_p^m(t) \approx h_p^m$ for the duration of one OFDM block. With these notions, we can rewrite (2) as

$$h_m(\tau, t) \approx \sum_p h_p^m \delta(\tau - \tau_p^m + at),\ m = 1, \ldots, M_r \tag{3}$$

where the path delays τ_p^m have a continuum of values.

After frame synchronization, initial resampling, which is performed based on the method proposed in [8], and down-conversion, the lowpass equivalent received signal on the mth receiving element is modeled as

$$v_m(t) = e^{i\beta t}\sum_{k=0}^{K-1} H_k^m d_k e^{2\pi i k\Delta f t} + w_m(t),\ t \in [0, T] \tag{4}$$

where β is the unknown frequency offset assumed common for all M_r receiving elements, and $w_m(t)$ is the additive noise. The channel frequency response on the kth carrier of the mth receiving elements H_k^m is given by

$$H_k^m = H_m(f_k) = \sum_p h_p^m e^{-2\pi i f_k \tau_p^m} = \sum_p c_p^m e^{-2\pi i k\Delta f \tau_p^m} \tag{5}$$

where $c_p^m = h_p^m e^{-2\pi i f_0 \tau_p^m}$. We refer to the model (5) as the physical propagation model (path-based model).

Assuming the same gross frequency offset β for all receiving elements is plausible when the elements are co-located, and it helps to promote the multichannel processing gain. The model (4) captures rough frequency shifting and serves as a starting point in developing the method for frequency offset compensation. The finer points of frequency shift changing across the bandwidth are left to post-FFT processing.

III. Practical Receiver Algorithms

Fig. 1 depicts the receiver processing for each receiving element. Next, we discuss the two key blocks, namely frequency offset estimation and channel estimation.

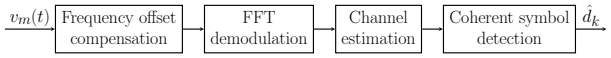

Fig. 1. Block diagram of the coherent OFDM receiver. The main building blocks of the receiver are the frequency offset estimation and channel estimation. The lowpass equivalent received signal $v_m(t)$ is obtained after frame synchronization, initial resampling, and downshifting and lowpass filtering. After compensating for the frequency offset, and estimating the channel coefficients, maximum ratio combining (MRC) yields the data symbol estimates $\hat{d}_k$.

A. Frequency Offset Estimation

Assuming that the M_r signals are compensated by some estimated value $\hat{\beta}$, demodulation is performed on all the carriers and receiving elements to yield

$$y_k^m(\hat{\beta}) = \frac{1}{T}\int_T v_m(t) e^{-i\hat{\beta}t} e^{-2\pi i k\Delta f t} dt \tag{6}$$

where $k = 0, \ldots, K-1$ and $m = 1, \ldots, M_r$. Arranging the signals corresponding to carrier k into a vector $\mathbf{y}_k$, and performing differential maximum ratio combining (DMRC), the estimates of the differentially-encoded data symbols $b_k = d_{k-1}^* d_k$ are obtained as [1]

$$\hat{b}_k(\hat{\beta}) = \frac{\mathbf{y}_{k-1}'(\hat{\beta})\mathbf{y}_k(\hat{\beta})}{\mathbf{y}_{k-1}'(\hat{\beta})\mathbf{y}_{k-1}(\hat{\beta})} \triangleq \frac{N_k(\hat{\beta})}{D_k(\hat{\beta})} \tag{7}$$

where we implicitly assume that the channel frequency response changes slowly from one carrier to the next, i.e. $H_{k-1}^m \approx H_k^m$, $\forall k = 1, \ldots, K-1$ and $m = 1, \ldots, M_r$.

The error in data symbol estimation is $e_k(\hat{\beta}) = b_k - \hat{b}_k(\hat{\beta})$. Using pilot data symbols that belong to a set of carriers $\mathcal{K}_p$, a composite error can be formed as $E(\hat{\beta}) = \sum_{k\in\mathcal{K}_p} |e_k(\hat{\beta})|^2$, and this error can be used to close the loop and guide the estimation of β. The task of the frequency offset estimation algorithm is to form an estimate of the frequency offset which will minimize the error in the mean square sense. This task will be accomplished when the composite error gradient is zero,

$$\frac{\partial \mathbb{E}\{E(\hat{\beta})\}}{\partial \hat{\beta}} = -2\mathbb{E}\{\Re\{\sum_{k\in\mathcal{K}_p}\frac{1}{D_k}[\dot{N}_k - \hat{b}_k\dot{D}_k]e_k^*\}\} = 0 \tag{8}$$

where dot denotes the derivative with respect to $\hat{\beta}$. Using the instantaneous value of this gradient $\gamma = -2\Re\{\sum_{k\in\mathcal{K}_p}[\dot{N}_k - \hat{b}_k\dot{D}_k]e_k^*/D_k\}$, $\hat{\beta}$ can be calculated iteratively as

$$\hat{\beta}(j+1) = \hat{\beta}(j) + K_\beta\gamma(j) \tag{9}$$

where K_β is the frequency offset update parameter. The initial point $\hat{\beta}(0)$ can be set to zero when the frequency offset $\beta/2\pi$ is a fraction of carrier spacing Δf. We will comment on the initial point and step size shortly. The algorithm can be set to run either for a prespecified maximum number of iterations N_I or a predefined error threshold η_f. Fig. 2 shows the signal flow of the frequency offset estimation block.

The performance of the stochastic gradient algorithm depends on the initial point $\hat{\beta}(0)$. Since the composite error is a

[1] $(\cdot)'$ denotes conjugate-transpose.

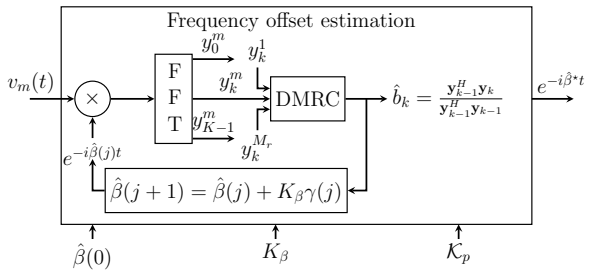

Fig. 2. Block diagram of the frequency offset estimation algorithm. The algorithm is based on differential encoding, and estimates the frequency offset iteratively based on a stochastic-gradient approach. $\mathcal{K}_p$ is the set of pilot carriers used to form the composite error $E(\hat{\beta})$. The total computational cost of the algorithm is upper-bounded by $O(2N_I M_r K \log(K))$, where N_I is the maximum number of iterations.

non-convex function of the frequency offset $\hat{\beta}$, yet has a global minimizer, the frequency offset estimation algorithm is prone to converge to a local minimum [8]. Thus, to obtain a proper initial point that precludes the algorithm from converging to local minima, the hypothesis testing approach, proposed in [4], is applied to the first block to start the process. Assuming that the frequency offset is changing slowly from one block to the next, for the second block and on, the initial value of the update (9) is set to the frequency offset estimated in the previous block.

Another factor on which the performance of the frequency offset estimation algorithm relies is the step size K_β which dictates the speed of convergence. The step size is automatically computed using the Barzilai-Borwein method [9]. For the iteration $j = 0$, $K_\beta(0)$ is set to a small value, e.g., 1, to preclude the algorithm from diverging.

B. Channel Estimation

After compensating for the frequency offset, and assuming that the frequency offset estimate $\hat{\beta}$ is close enough to the true value, one can assume that there is no inter-carrier interference, such that the demodulator outputs can be modeled as

$$y_k^m = d_k H_k^m + z_k^m \tag{10}$$

where H_k^m are the channel coefficients and z_k^m are the noise components. Assuming without the loss of generality that all K data symbols are available for channel estimation (e.g. correct symbol decisions, or all-pilots in an initial block), the input to the channel estimator is given by $x_k^m = y_k^m / d_k$, i.e.

$$\mathbf{x}^m = \mathbf{H}^m + \mathbf{z}^m,\ m = 1, \ldots, M_r \tag{11}$$

where $\mathbf{H}^m = \sum_p c_p \mathbf{s}_K(2\pi\Delta f \tau_p)$ and $\mathbf{z}^m$ represents an equivalent noise vector. The vector $\mathbf{s}_K(2\pi\Delta f\tau) = \begin{bmatrix}1 & e^{-2\pi i \Delta f \tau} & \cdots & e^{-2\pi i (K-1)\Delta f \tau}\end{bmatrix}^T$ is referred to as the steering vector at an arbitrary delay τ.

Consider now the following operation performed on the noisy channel observation $\mathbf{x}^m$ at the mth receiving element:

$$\begin{aligned} r_m(\tau) &= \frac{1}{K} \mathbf{s}_K^H(2\pi\Delta f\tau)\mathbf{x}^m \\ &= \sum_p c_p^m g_K\left(2\pi\Delta f(\tau - \tau_p^m)\right) + w_m(\tau),\ \tau \in \tau_{obs} \end{aligned} \tag{12}$$

where $g_K(\varphi) = \frac{1}{K}\sum_{k=0}^{K-1} e^{ik\varphi}$ is a known signature function, and $w_m(\tau)$ is the corresponding complex noise. The interval τ_{obs} is a preset interval that captures the multipath spread. In a digital implementation, an arbitrary resolution is used, e.g. $\Delta\tau = T/IK$, where I represents the resolution factor, i.e. the increase in resolution over the standard sample spacing $1/B = T/K$. The total length of the observation interval is $L = \lceil T_g B \rceil$, where T_g is the guard interval which is at least as long as the multipath spread.

The signal $r_m(\tau)$ serves as the input to the PI algorithm. The algorithm operates recursively, identifying at each iteration the delay of the next-strongest path in a manner similar to matching pursuit. The algorithm can be set to run either for a prespecified number of channel paths N_P (sparsity level) or a predefined residual error threshold η_c.

The formal steps of the PI algorithm are summarized in Algorithm 1. The last step of the algorithm represents a refinement in which a least squares problem is solved for possible improvement in estimating the path gains c_p^m. This step is optional. The total complexity of the PI algorithm is $O(ILK) + O(N_P IL) + O(KN_P^2)$ [7].

Algorithm 1 PI algorithm

Input: $\mathbf{x}^m$, N_P (or η_c)
Output: $\hat{\mathbf{H}}^m$

$r^{(0)}(\tau) = r_m(\tau)$ {*initialization step*}
while $p \le N_P$ (or $|r^{(p)}(\tau)| > \eta \max_\tau |r_m(\tau)|$) **do**
  $\hat{\tau}_p^m = \arg\max_\tau |r^{(p)}(\tau)|$
  $\hat{c}_p^m = r^{(p)}(\hat{\tau}_p^m)$
  $r^{(p+1)}(\tau) = r^{(p)}(\tau) - \hat{c}_p^m g_K\left(2\pi\Delta f(\tau - \hat{\tau}_p^m)\right)$
end while
$\hat{\mathbf{S}}_m = \begin{bmatrix}\mathbf{s}_K(2\pi\Delta f\hat{\tau}_1^m) & \cdots & \mathbf{s}_K(2\pi\Delta f\hat{\tau}_{N_P}^m)\end{bmatrix}$
$\hat{\mathbf{c}}^m = \left(\hat{\mathbf{S}}_m'\hat{\mathbf{S}}_m\right)^{-1}\hat{\mathbf{S}}_m'\mathbf{x}^m$ {*refinement step*}
return $\hat{\mathbf{H}}^m = \hat{\mathbf{S}}_m\hat{\mathbf{c}}^m$

Using the model (10) yields the M_r-element received signal vector $\mathbf{y}_k = d_k\mathbf{H}_k + \mathbf{z}_k,\ k = 0, \ldots, K-1$ where $\mathbf{H}_k$ and $\mathbf{z}_k$ contain the relevant channel and noise components, respectively. Assuming that the channels observed across the receiver array are uncorrelated, maximum ratio combining (MRC) finally yields the data estimate

$$\hat{d}_k = \frac{\hat{\mathbf{H}}_k'\mathbf{y}_k}{\|\hat{\mathbf{H}}_k\|_2^2},\ k = 0, \ldots, K-1 \tag{13}$$

IV. Experimental Result

To asses the system performance, we focus on the experimental data from the Mobile Acoustic Communication Experiment (MACE'10) which took place off the coast of Martha's Vineyard, Massachusetts, in June 2010. The experimental signals, whose parameters are given in Table I, were transmitted using the acoustic frequency range between 10.5 kHz and 15.5 kHz. The receiver array of 12 equally-spaced elements spanning a total linear aperture of 1.32 m was suspended at the depth of 40 m and the transmitter was towed at the depth of 40-60 m. The water depth was approximately

100 m, and the transmission distance varied between 3 km and 7 km.

The experiment consisted of multiple repeated transmissions, each containing all the OFDM signals listed in Table I. There was a total of 52 transmissions spanning 3.5 hours of recording. During this time, the transmitting station moved away and towards the receiving station, at varying speeds ranging from 0.5 m/s to 1.5 m/s. The results provided in this section are obtained from all 52 transmissions.

TABLE I
MACE'10 SIGNAL PARAMETERS.

number of carriers K	1024
modulation	8-PSK
number of blocks per frame N_B	8
carrier spacing Δf [Hz]	4.8
bit rate [kbps]	12
bandwidth efficiency [bps/Hz]	2.4

The guard interval is $T_g = 16$ msec. The bandwidth efficiency is calculated assuming 136 pilots for coherent data detection, out of which only 8 pairs of adjacent carriers are used for frequency offset estimation.

We illustrate the performance of the proposed receiver on an exemplary OFDM frame from the MACE'10 experiment. In Fig. 3, we illustrate the receiver operation on one OFDM frame containing 8 blocks each with $K = 1024$ carriers modulated by 8-PSK data symbols. Shown are the frequency offset estimate for the 8 blocks in the underlying frame, the evolution of the instantaneous gradient $\gamma(j)$, algorithm convergence plot obtained for the last block in the frame, the channel frequency and impulse responses seen on the 12 available receiving elements, and the last block's scatter plot.

Due to the random channel variation and a finite number of measurements, the data detection MSE is a random variable. Thus, we demonstrate the performance of the system in terms of the estimated cumulative density function (CDF) of the data detection MSE measured in each signal frame. Furthermore, we show the bit error rate (BER) of the system when low-density parity check (LDPC) codes are used with various code rates. We also compare the coherent receiver discussed in this paper with two differentially-coherent receivers, namely, one with frequency offset estimation and one without that.

Fig. 4 illustrates the estimated cumulative density function of the MSE per block. This result refers to $K = 1024$ carries and includes all the frames, transmitted over 3.5 hours. The coherent receiver equipped with the algorithms discussed in this paper delivers MSE below -14 dB for 90% of the OFDM blocks conveying 8-PSK symbols. Fig. 4 also shows that the coherent receiver outperforms the differentially-coherent receiver which uses the same algorithm for frequency offset compensation. Fig. 4 also accentuates the key role that estimating motion-induced frequency offsets plays in successfully detecting data symbols.

Finally, in Fig. 5 we address the performance of the system in which regular low-density parity check (LDPC) codes are used. We consider various code rates ranging from 0.1 to 1, and evaluate the system performance in terms of the average bit error rate (BER). We use soft decision decoding that takes the likelihood ratio for each code-bit as an input. Decoding is performed based on the probability propagation algorithm which can be seen as an instance of the sum-product algorithm [10]. The stochastic gradient algorithm for frequency offset estimation and the PI algorithm for channel estimation enable LDPC to work to its full potential. With code rate as high as 0.7, the coherent receiver achieves the BER of 2×10^{-5}. Lower code rates resulted in no errors measurable with the data at hand.

V. CONCLUSION

We considered coherent detection of acoustic OFDM signals passed through mobile acoustic channels. We targeted the frequency offset through a stochastic gradient algorithm that is based on differential encoding, keeping the complexity of the receiver at a minimum. The key feature of the algorithm is that only a few pilots suffice to determine the frequency shift. We also investigated a sparse channel estimation method, path identification, that operates on the transformed version of the input signal to identify the dominant propagation paths. Unlike the conventional sample-space channel estimation methods, path identification considers a continuum of delays and allows for increasing the delay resolution without undue penalty on complexity.

We presented a statistical performance analysis using experimental signals recorded over a mobile acoustic channel. Our results show that the proposed coherent receiver delivers an average MSE below -14 dB for 90% of OFDM blocks and enables a very high rate LDPC code to achieve an excellent BER of 5×10^{-5} at very low computational complexity.

REFERENCES

[1] B. Li, S. Zhou, M. Stojanovic, L. Freitag, and P. Willett, "Multicarrier communication over underwater acoustic channels with nonuniform Doppler shifts," *IEEE J. Ocean. Eng.*, vol. 33, no. 2, pp. 198–209, Apr. 2008.

[2] K. Tu, T. M. Duman, M. Stojanovic, and J. G. Proakis, "Multiple-resampling receiver design for OFDM over Doppler-distorted underwater acoustic channels," *IEEE J. Ocean. Eng.*, vol. 38, no. 2, pp. 333–346, Apr. 2013.

[3] Y. M. Aval and M. Stojanovic, "Differentially coherent multichannel detection of acoustic OFDM signals," *IEEE J. Ocean. Eng.*, vol. 40, no. 2, pp. 251–268, Apr. 2015.

[4] A. Tadayon and M. Stojanovic, "Frequency offset compensation for acoustic OFDM systems," in *Proc. IEEE OCEANS 2017 Conf.*, Anchorage, AK, pp. 1–5.

[5] C. R. Berger, S. Zhou, J. C. Preisig, and P. Willett, "Sparse channel estimation for multicarrier underwater acoustic communication: From subspace methods to compressed sensing," *IEEE Trans. Signal Process.*, vol. 58, no. 3, pp. 1708–1721, Mar. 2010.

[6] A. Radosevic, R. Ahmed, T. M. Duman, J. G. Proakis, and M. Stojanovic, "Adaptive OFDM modulation for underwater acoustic communications: Design considerations and experimental results," *IEEE J. Ocean. Eng.*, vol. 39, no. 2, pp. 357–370, Apr. 2014.

[7] A. Tadayon and M. Stojanovic, "Path-based channel estimation for acoustic OFDM systems: Real data analysis," in *Proc. 51st Asilomar Conf. on Signals, Sys., and Comput.*, Oct. 2017, pp. 1759–1763.

[8] A. Tadayon and M. Stojanovic, "Low-complexity superresolution frequency offset estimation for high data rate acoustic OFDM systems," *IEEE J. Ocean. Eng.*, pp. 1–11, 2018.

[9] J. Barzilai and J. M. Borwein, "Two-point step size gradient methods," *IMA J. Numer. Anal.*, vol. 8, no. 1, pp. 141–148, 1988.

[10] D. J. MacKay, "Good error-correcting codes based on very sparse matrices," *IEEE Trans. Inf. Theory*, vol. 45, no. 2, pp. 399–431, Mar. 1999.

[11] W. Ryan and S. Lin, *Channel codes: classical and modern*. Cambridge University Press, 2009.

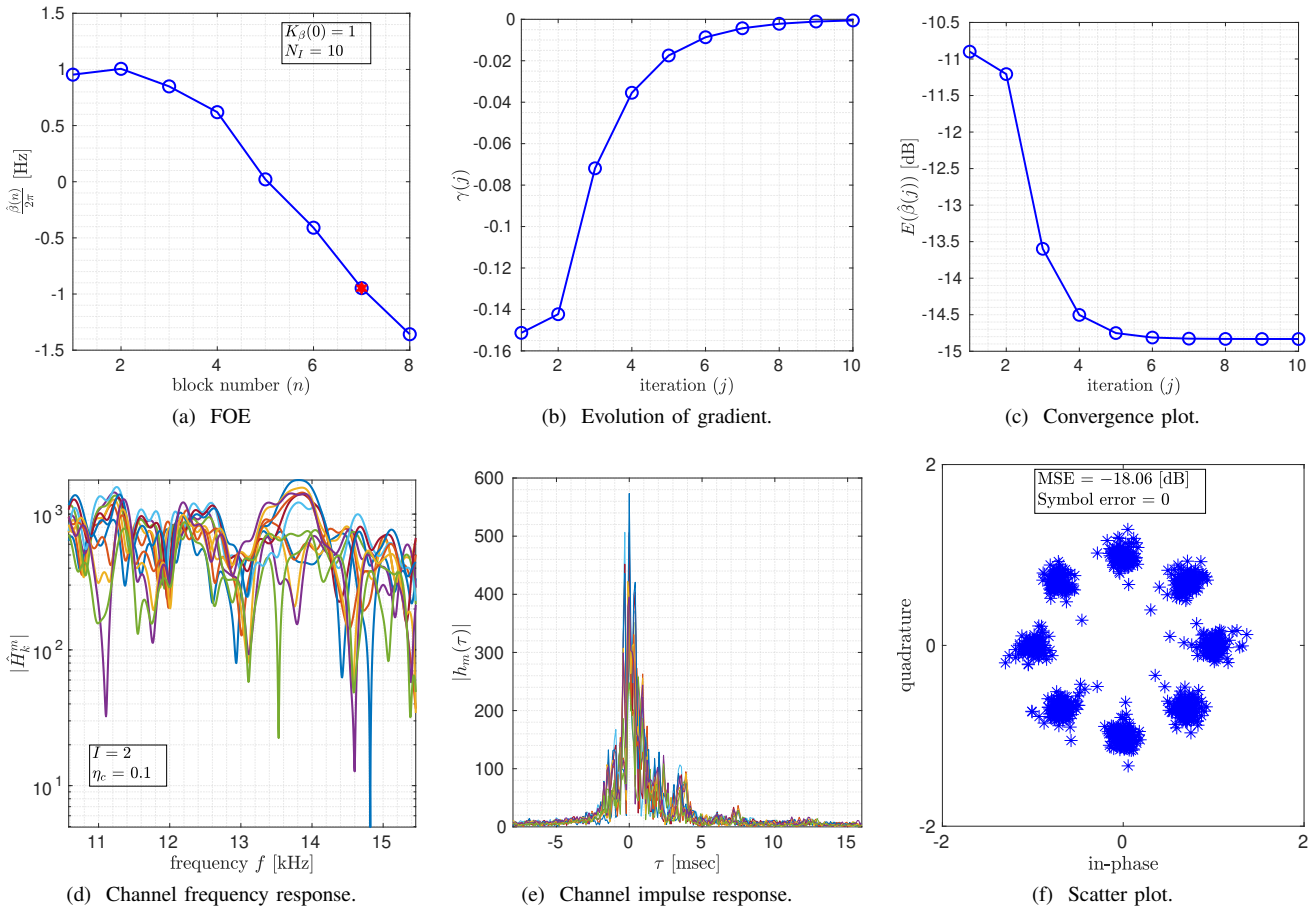

(a) FOE (b) Evolution of gradient. (c) Convergence plot.

(d) Channel frequency response. (e) Channel impulse response. (f) Scatter plot.

Fig. 3. Performance illustration for an OFDM frame with 8 blocks and $K = 1024$ carriers modulated by 8-PSK data symbols. Shown are the frequency offset estimate for the entire frame, the evolution of the gradient $\gamma(j)$ for the last block, the algorithm convergence plot obtained for the last block, the estimates of channel frequency response and channel impulse response, and the last block's scatter plot. The total number of pilots used to perform the frequency offset and channel estimation is 136, out of which only 8 differentially-encoded pilots are used to do frequency offset estimation. The hypothesis testing approach is applied to the first block. For the second block and on, the initial value of the update (9) is set to the frequency offset estimated in the previous block (shown in (a) with colored circle). The step size K_β is set to 1 in the first iteration and then updated using the Barzilai-Borwein method. For the PI, the resolution factor I and the threshold η_c are set to 2 and 0.1, respectively. In the last block, the data detection MSE is -18 dB and there are no symbols errors.

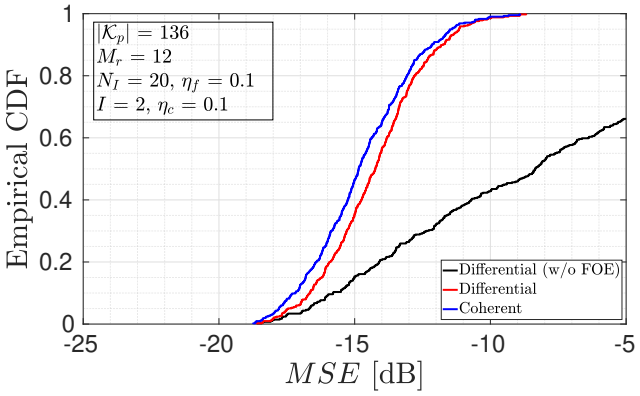

Fig. 4. The estimated CDF of the data detection MSE. The CDFs reflect all 52 transmission with $K = 1024$ carriers during MACE'10. For frequency offset estimation, the stochastic gradient algorithm terminates if the absolute difference between composite errors in two consecutive iterations is less than $\eta_f = 0.1$. While the differentially-coherent receiver delivers MSE below -12 dB for 90% of block, the coherent receiver delivers MSE below -14 dB with the same level of reliability. The performance of the coherent and differentially-coherent receivers equipped with the frequency offset estimation algorithm is compared to that of the differentially-coherent receiver without any frequency offset estimation (w/o FOE). Clearly, FOE is essential to proper operation.

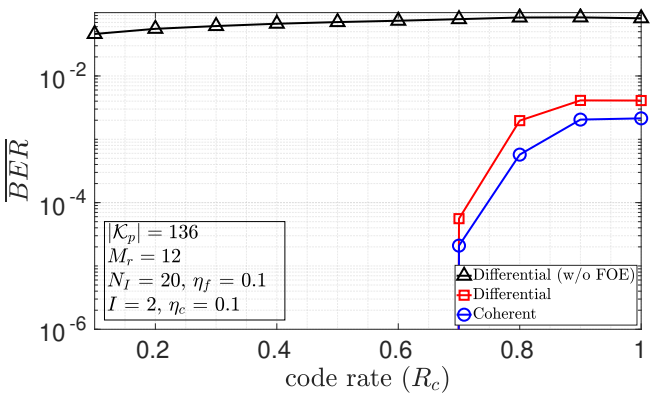

Fig. 5. Average BER versus the rate of the LDPC code. The codeword length is $N = 3K$; thus, each codeword constitutes an OFDM block. The column weight of the $M \times N$ parity check matrix (M is the number of parity bits) is $w_c = 3$ for all the code rates considered, and the row weight $w_r = w_c N/M$ varies from 3.3 to 30, corresponding to the code rates ranging from 0.1 to 0.9 [11]. The results reflect all 52 transmissions of blocks with 1024 carriers during MACE'10. Using code rates as high as 1, the coherent detection enables excellent performance with BER $= 2\times10^{-3}$ for ZP-OFDM blocks whose carriers are 8-PSK modulated. Code rates below 0.7 result in low BER values that cannot be measured with the existing data.